

# Determination of gluon polarization from deep inelastic scattering and collider data

M. Hirai<sup>1,2,3</sup> and S. Kumano<sup>4,5</sup>

<sup>1</sup>*Department of Physics, Tokyo Institute of Technology, Meguro, Tokyo, 152-8551, Japan*

<sup>2</sup>*Department of Physics, Juntendo University, Inba, Chiba, 270-1695, Japan*

<sup>3</sup>*Department of Physics, Tokyo University of Science, Noda, Chiba 278-8510, Japan*

<sup>4</sup>*Institute of Particle and Nuclear Studies, High Energy Accelerator Research Organization (KEK)  
1-1, Ooho, Tsukuba, Ibaraki, 305-0801, Japan*

<sup>5</sup>*Department of Particle and Nuclear Studies, Graduate University for Advanced Studies  
1-1, Ooho, Tsukuba, Ibaraki, 305-0801, Japan*

(Dated: November 27, 2008)

We investigate impact of  $\pi^0$ -production data at Relativistic Heavy Ion Collider (RHIC) and future E07-011 experiment for the structure function  $g_1$  of the deuteron at the Thomas Jefferson National Accelerator Facility (JLab) on studies of nucleonic spin structure, especially on the polarized gluon distribution function. By global analyses of polarized lepton-nucleon scattering and the  $\pi^0$ -production data, polarized parton distribution functions are determined and their uncertainties are estimated by the Hessian method. Two types of the gluon distribution function are investigated. One is a positive distribution and the other is a node-type distribution which changes sign at  $x \sim 0.1$ . Although the RHIC  $\pi^0$  data seem to favor the node type for  $\Delta g(x)$ , it is difficult to determine a precise functional form from the current data. However, it is interesting to find that the gluon distribution  $\Delta g(x)$  is positive at large  $x$  ( $> 0.2$ ) due to constraints from the scaling violation in  $g_1$  and RHIC  $\pi^0$  data. The JLab-E07-011 measurements for  $g_1^d$  should be also able to reduce the gluon uncertainty, and the reduction is comparable to the one by RUN-5  $\pi^0$ -production data at RHIC. The reduction is caused mainly by the error correlation between polarized antiquark and gluon distributions and by a next-to-leading-order (NLO) gluonic effect in the structure function  $g_1^d$ . We find that the JLab-E07-011 data are accurate enough to probe the NLO gluonic term in  $g_1$ . Both RHIC and JLab data contribute to better determination of the polarized gluon distribution in addition to improvement on polarized quark and antiquark distributions.

PACS numbers: 13.60.Hb, 13.88.+e

## I. INTRODUCTION

Quark and gluon contributions to the nucleon spin are described by polarized parton distribution functions (polarized PDFs) and their first moments. It became clear that only a small fraction of nucleon spin is carried by quarks and antiquarks. Therefore, a large gluon polarization or effects of orbital angular momenta should be possible sources for explaining the origin of the nucleon spin. The gluon polarization is expected to be clarified in the near future, whereas it would take time to determine the effects of the orbital angular momenta.

Polarized PDFs have been investigated by global analyses of data on polarized lepton-nucleon deep inelastic scattering (DIS) and proton-proton collisions [1, 2, 3, 4, 5, 6]. Polarized quark distributions are determined relatively well; however, the polarized gluon distribution  $\Delta g(x)$  is not accurately determined. Here,  $x$  is the Bjorken scaling variable, and  $\Delta g(x)$  is the difference between the gluon distribution with helicity parallel to that of parent nucleon and the one with helicity anti-parallel.

The gluon distribution contributes to the structure function  $g_1$  as a higher-order effect in the expansion by the running coupling constant  $\alpha_s$  of quantum chromodynamics. The unpolarized gluon distribution has been determined primarily by the  $Q^2$  dependence of  $F_2$  at small

$x$ , where  $Q^2$  is defined by the momentum transfer  $q$  by  $Q^2 = -q^2$  in lepton scattering. The kinematical range of  $x$  and  $Q^2$  is still limited for  $g_1$  in determining  $\Delta g(x)$  by the scaling violation, so that the determination of  $\Delta g(x)$  is difficult from the scaling violation. Nonetheless, it is noteworthy that there are  $Q^2$  differences between the COMPASS and HERMES data for  $g_1$  in the range of  $x \sim 0.05$ . Such  $Q^2$  differences could be used for constraining a gluon polarization at large  $x$  as pointed out in Ref. [5]. However, this idea should be tested by future measurements on the scaling violation in  $g_1$  because the  $Q^2$  differences could originate also from higher-twist effects [3].

Other types of measurements are needed to improve the situation of  $\Delta g(x)$ . There were measurements on  $\Delta g(x)$  in lepton-nucleon scattering by observing high- $p_T$  hadrons [7, 8, 9] and open-charm events [10]. These data provided constraints on the gluon polarization at  $x \sim 0.1$ . They indicated that the ratio  $\Delta g(x)/g(x)$  is small although experimental errors are still large. Measurements at Relativistic Heavy Ion Collider (RHIC) are also important for constraining the gluon polarization. For example,  $\pi^0$  and jet-production data [11, 12] in polarized proton-proton collisions are valuable for the determination of  $\Delta g(x)$ . In fact, we showed that the  $\pi^0$  data play an important role in reducing the uncertainty

of  $\Delta g(x)$  by a global analysis including the  $\pi^0$  data in addition to the DIS data [5]. Certain fragmentation functions are used in the analysis of  $\pi^0$ -production processes. We should be careful that gluon and light-quark fragmentation functions have large uncertainties at small  $Q^2$  or small  $p_T$  [13].

In order to determine the polarized PDFs including the gluon polarization, precise measurements are needed also in DIS. After our previous analysis [5], new DIS data are reported by the CLAS [14], HERMES [15], and COMPASS [16] collaborations. In future, the structure function  $g_1$  for the deuteron will be accurately measured at the Thomas Jefferson National Accelerator Facility (JLab) by the proposed experiment E07-011 [17, 18]. The measurements at JLab should be valuable for reducing large uncertainties of the polarized antiquark and gluon distributions because they cover a large- $x$  region at small  $Q^2$ .

In this work, we determine the polarized PDFs by global analyses of the data for spin asymmetries  $A_1$  in polarized lepton-nucleon DIS and double spin asymmetries  $A_{LL}$  of the  $\pi^0$  production in proton-proton collisions. In particular, we focus our discussions on determination of the polarized gluon distribution function. The purposes of this article are the following.

- (1) The RHIC  $\pi^0$ -production data could indicate a node-type distribution for  $\Delta g(x)$ , so that two types of distributions are studied in the global analysis by taking a positive distribution for  $\Delta g(x)$  and a node-type distribution which changes sign at  $x \sim 0.1$ .
- (2) Among various future experimental projects, we investigate impact on the polarized PDFs, especially on the polarized gluon distribution function, from precise measurements on the structure function  $g_1$  of the deuteron by the JLab-E07-011 experiment [17, 18]. The E07-011 data will be so precise that  $\Delta g(x)$  could be constrained.
- (3) The polarized PDFs obtained with the E07-011 data are compared with the ones including the  $\pi^0$ -production data especially in reducing uncertainties of  $\Delta g(x)$  and its first moment.

We provide a new AAC08 (Asymmetry Analysis Collaboration in 2008) library by the current global analyses because updated AAC distributions have not been provided since the 2003 version [4, 19].

This article is organized as follows. In Sec. II, three data sets are introduced for investigating roles of the RHIC  $\pi^0$  and JLab data, and our analysis method is explained. Analysis results are discussed in Sec. III, and they are summarized in Sec. IV.

## II. ANALYSIS METHOD

In order to investigate roles of the RHIC  $\pi^0$  and E07-011 data, three data sets in Table I are prepared. The

TABLE I: Used data sets in our global analyses. The ‘‘DIS’’ indicates current DIS data on  $g_1$ . The RHIC  $\pi^0$  data are taken from Ref. [11]. The JLab-E07-011 data are calculated by using estimated errors in Refs. [17, 18] and set-A results, and actual values are shown in Table II. The notation  $\bigcirc$  indicates an included data set.

Analysis set	DIS	RHIC $\pi^0$	E07-011
A	$\bigcirc$	–	–
B	$\bigcirc$	$\bigcirc$	–
C	$\bigcirc$	–	$\bigcirc$

notation ‘‘DIS’’ indicates all the present DIS data on  $g_1$ , and they are almost the same data used in the AAC06 analysis [5]. There are minor changes. The same data are used for SLAC, EMC, SMC, and HERMES; however, updated ones are used for the deuteron by the COMPASS [16]. In addition, the CLAS data [14] are included in the DIS set. This is called set A; the one with  $\pi^0$  data is set B; the one with the E07-011 is set C. The data for the RHIC  $\pi^0$  and expected E07-011 are taken from Refs. [11] and [17, 18], respectively. The RUN-5 data are used for the  $\pi^0$  production. Preliminary RUN-6 data by the PHENIX collaboration [20] and jet data of the STAR collaboration [12] are not included in our analyses. We may include these data in our future global analysis. Comparing three analysis results, we try to clarify roles of the RHIC  $\pi^0$  and E07-011 data in the determination of the polarized PDFs, especially on  $\Delta g(x)$ , in comparison with the results by the set A.

The expected data for  $A_1^d$  of the E07-011 experiment are estimated in the following way. The asymmetries are assumed to be the same as the ones of the analysis A:  $A_1^d(x, Q^2)_{\text{E07-011}} \equiv A_1^d(x, Q^2)_{\text{set-A}}$ . Expected errors of the E07-011 experiment are estimated for  $(\delta g_1^d/g_1^d)_{\text{E07-011}}$  in the proposal [17, 18], and they are converted to the errors of  $A_1^d$  by

$$\delta A_1^d(x, Q^2)_{\text{E07-011}} \equiv \left[ \frac{\delta g_1^d(x, Q^2)}{g_1^d(x, Q^2)} \right]_{\text{E07-011}} A_1^d(x, Q^2)_{\text{set-A}}. \quad (1)$$

Estimated values and their errors are shown for the asymmetry  $A_1^d(x, Q^2)$  in Table II. It should be noted that there are two solutions for the polarized PDFs, the positive and node-type distributions, so that there are two sets of  $A_1^d$  data in Table II.

The kinematical region of the used DIS data for proton, neutron, and deuteron is shown in Fig. 1 by  $x$  and  $Q^2$ . The CERN data (EMC, SMC, COMPASS) cover a wide  $x$  region with relatively large  $Q^2$ . The are especially important for determining the polarized PDFs at small  $x$  ( $x \sim 0.01$ ). The SLAC (E130, E142, E143, E154, E155), DESY (HERMES), and JLab (Hall-A, CLAS, E07-011) data are at relatively large  $x$  with small  $Q^2$ . The are especially important for determining the polarized PDFs at large  $x$  and also possibly the polarized gluon distribution in comparison with the CERN data.

TABLE II: Expected asymmetries  $A_1^d(x, Q^2)$  and their errors in the E07-011 experiment. They are calculated by using the set-A analysis results and estimated errors  $\delta g_1^d/g_1^d$ . The details are explained in the text.

$x$	$Q^2$ (GeV <sup>2</sup> )	$\delta g_1^d/g_1^d$	$A_1^d$		$\delta A_1^d$	
			positive	node		
0.175	1.4	0.020	0.0841	0.0017	0.0819	0.0016
0.25	1.9	0.014	0.1568	0.0022	0.1475	0.0021
0.35	2.5	0.010	0.2522	0.0025	0.2453	0.0025
0.45	3.0	0.010	0.3416	0.0034	0.3414	0.0034
0.55	3.7	0.015	0.4308	0.0065	0.4384	0.0066

The details of our analysis method are explained in our previous article [5], so that only a brief outline is explained in the following. The polarized PDFs are given at the initial  $Q^2$  scale ( $\equiv Q_0^2$ ), where it is taken  $Q_0^2 = 1$  GeV<sup>2</sup>, with a number of parameters:

$$\Delta f(x, Q_0^2) = [\delta x^\nu - \kappa(x^\nu - x^\mu)]f(x, Q_0^2), \quad (2)$$

where  $\delta$ ,  $\kappa$ ,  $\nu$ , and  $\mu$  are parameters to be determined by a  $\chi^2$  analysis, and  $f(x)$  is the corresponding unpolarized PDF [21]. Flavor symmetric antiquark distributions are assumed for the polarized PDFs at the initial scale although the unpolarized antiquark distributions are not flavor symmetric [22]. They are evolved to experimental  $Q^2$  points by the DGLAP (Dokshitzer-Gribov-Lipatov-Altarelli-Parisi) equations [23].

The parameters are then determined by a  $\chi^2$  analysis of experimental data on spin asymmetries so as to minimize

$$\chi^2 = \sum_i \frac{[A_i^{\text{data}}(x, Q^2) - A_i^{\text{calc}}(x, Q^2)]^2}{[\Delta A_i^{\text{data}}(x, Q^2)]^2}. \quad (3)$$

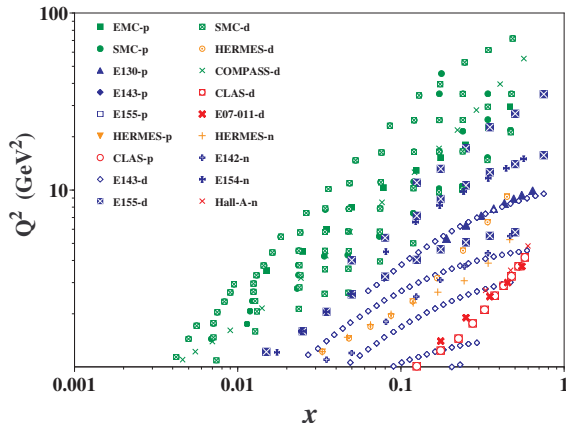


FIG. 1: Kinematical region of the DIS data is shown by  $x$  and  $Q^2$ . The notations  $p$ ,  $n$ , and  $d$  indicate proton, neutron, and deuteron, respectively.

Here, the spin asymmetries are  $A_1$  in the DIS and  $A_{LL}^{\pi^0}$  in the  $\pi^0$  production. The analyses are done in the next-to-leading order (NLO) of the running coupling constant  $\alpha_s$ , and the modified minimal subtraction ( $\overline{\text{MS}}$ ) scheme is used. The fragmentation functions of the HKNS07 (Hirai, Kumano, Nagai, Sudoh in 2007) [13] are used for describing the fragmentation into the pion. However, uncertainties of the fragmentation functions are not included in this analysis. The uncertainties of the polarized PDFs are estimated by the Hessian method:

$$[\delta F(x)]^2 = \Delta\chi^2 \sum_{i,j} \left( \frac{\partial F(x, a)}{\partial a_i} \right)_{a=\hat{a}} H_{ij}^{-1} \left( \frac{\partial F(x, a)}{\partial a_j} \right)_{a=\hat{a}}, \quad (4)$$

where  $F(x)$  is a polarized PDF,  $H_{ij}$  is the Hessian, the parameters are denoted  $a_i$  ( $i=1, 2, \dots, N$ ), and  $\hat{a}$  indicates the parameter set at the minimum  $\chi^2$  point. The value of  $\Delta\chi^2$  is taken as  $\Delta\chi^2 = 12.65$  so that the uncertainty indicates the one- $\sigma$ -error range for the normal distribution in the eleven-parameter space [4, 5]. The details of the analysis conditions and the uncertainty-estimation method are found in Ref. [5].

We comment on our choice of  $\Delta\chi^2$ . As explained in Ref. [24],  $\Delta\chi^2 \sim N$  gives one- $\sigma$  error for a multivariate normal distribution of fit parameters. We took this  $\Delta\chi^2$  value for estimating the uncertainties by considering it as an appropriate quantity for showing errors of overall functional behavior. However, this choice is not unique in global analyses of PDFs [16, 25]. For example,  $\Delta\chi^2 = 1$  is chosen in the COMPASS analysis for  $\Delta g(x)$  [16]. The difference between the choices,  $\Delta\chi^2 \sim N$  and  $\Delta\chi^2 = 1$ , comes from the fact that the likelihood function in the multiparameter space is different from the likelihood function for a physics quantity, for example,  $A_1(x, Q^2)$  at a fixed kinematical point of  $x$  and  $Q^2$ . If the latter likelihood is plotted as a function of this physical quantity (one degree of freedom)  $A_1(x, Q^2)$ , the one- $\sigma$  (68%) range as the statistical error of the function corresponds to the  $\Delta\chi^2 = 1$  region. However, our experience indicates that the choice  $\Delta\chi^2 = 1$  could be an underestimation of the uncertainties in comparison with experimental errors and their variations (see Figs. 1 and 3 in Ref. [5]). Therefore, CTEQ (Coordinated Theoretical/Experimental Project on QCD Phenomenology and Tests of the Standard Model) and MRST (Martin-Roberts-Stirling-Thorne) use larger  $\Delta\chi^2$  values ( $\Delta\chi^2 = 50$  or  $100$ ) [25] as an effective way to show the error range. Our choice  $\Delta\chi^2 \sim N$  is a conservative estimation of the uncertainty range by considering error correlations among the parameters. If one would like to use the choice  $\Delta\chi^2 = 1$ , one may scale down our polarized PDF uncertainties by  $1/\sqrt{\Delta\chi^2}$ .

### III. RESULTS

Three types of analyses are done with the different data sets in Table I. The  $\chi^2$  values are shown for each

TABLE III: Numbers of data and  $\chi^2$  values are listed for the three analysis sets with the data in Table I. The positive and node indicate a positive distribution and a node-type one, respectively, for  $\Delta g(x)$ . The notations  $p$ ,  $n$ , and  $d$  indicate proton, neutron, and deuteron, respectively.

Data set	No. of data	$\chi^2$					
		Set A		Set B		Set C	
		Positive	Node	Positive	Node	Positive	Node
EMC ( $p$ )	10	5.17	4.52	5.18	4.57	5.17	4.52
SMC ( $p$ )	59	56.34	53.79	56.77	53.95	56.34	53.79
E130 ( $p$ )	8	5.13	4.84	5.23	4.97	5.13	4.84
E143 ( $p$ )	81	59.97	59.78	60.43	60.30	59.97	59.78
E155 ( $p$ )	24	33.07	27.38	31.76	26.19	33.06	27.39
HERMES ( $p$ )	9	3.58	3.69	3.59	3.68	3.58	3.69
CLAS ( $p$ )	10	14.34	15.11	17.81	21.65	14.32	15.10
SMC ( $d$ )	65	57.39	56.65	57.82	56.86	57.39	56.65
E143 ( $d$ )	81	91.15	91.86	89.84	89.85	91.16	91.87
E155 ( $d$ )	24	18.60	22.44	18.53	23.32	18.60	22.44
HERMES ( $d$ )	9	11.19	8.10	11.93	7.65	11.20	8.10
COMPASS ( $d$ )	15	8.73	10.49	9.30	11.89	8.73	10.49
CLAS ( $d$ )	10	5.73	4.76	5.55	5.53	5.73	4.76
E07-011 ( $d$ )	5	–	–	–	–	0.00	0.00
E142 ( $n$ )	8	2.60	2.48	2.78	2.68	2.60	2.48
E154 ( $n$ )	11	3.32	4.09	3.07	3.12	3.32	4.10
HERMES ( $n$ )	9	2.26	2.41	2.18	2.36	2.26	2.41
Hall-A ( $n$ )	3	3.09	3.49	2.89	2.70	3.09	3.48
DIS total	441	381.66	375.87	384.65	381.27	381.66	375.87
PHENIX ( $\pi^0$ )	10	–	–	12.43	11.32	–	–
Total	451	381.66	375.87	397.08	392.60	381.66	375.87
( $\chi^2$ /d.o.f.)		(0.90)	(0.88)	(0.91)	(0.90)	(0.89)	(0.87)

TABLE IV: First moment of the polarized gluon distribution function and quark spin content  $\Delta\Sigma = \sum_i \int_0^1 dx [\Delta q_i(x) + \Delta \bar{q}_i(x)]$  at  $Q^2 = 1 \text{ GeV}^2$ .

	Set A		Set B		Set C	
	Positive	Node	Positive	Node	Positive	Node
$\Delta\Sigma$	$0.24 \pm 0.07$	$0.22 \pm 0.08$	$0.26 \pm 0.06$	$0.25 \pm 0.07$	$0.24 \pm 0.05$	$0.22 \pm 0.05$
$\Delta G$	$0.63 \pm 0.81$	$0.94 \pm 1.66$	$0.40 \pm 0.28$	$-0.12 \pm 1.78$	$0.63 \pm 0.45$	$0.94 \pm 1.09$

analysis in Table III. The total  $\chi^2$  values per degrees of freedom are in the range  $\chi^2/\text{d.o.f.} = 0.87 - 0.91$ , so that all the analyses are successful in explaining the data. The  $\chi^2$  value for the expected E07-011 data in the analysis C is very small ( $\sim 10^{-4}$ ) because the values of the data

TABLE V: The first moment  $\Delta G$  and its uncertainty  $\delta\Delta G$  at  $Q^2 = 1 \text{ GeV}^2$  in the range  $0.1 < x < 1$ . Here, the integrals are calculated in the limited  $x$  range by  $\Delta G(x > 0.1) \equiv \int_{0.1}^1 dx \Delta g(x)$ .

Function	Set	$\Delta G(x > 0.1)$	$\delta\Delta G(x > 0.1)$	$\frac{\delta\Delta G(x > 0.1)}{\Delta G(x > 0.1)}$
Positive	A	0.53	0.72	1.36
	B	0.36	0.26	0.71
	C	0.53	0.38	0.73
Node	A	0.87	0.89	1.02
	B	0.40	0.31	0.77
	C	0.87	0.47	0.54

are taken from the analysis-A results and there are no statistical variations. The polarized PDFs of the analysis C should be close to the ones of the analysis A. Comparison between A and C results is useful for discussing constraints from the E07-011 data on  $\Delta g(x)$  determination by noting differences between their uncertainties. First moments of the polarized PDFs are listed in Table IV. The first moments of  $\Delta u_v(x)$  and  $\Delta d_v(x)$  are fixed by semileptonic decays:  $\int_0^1 dx \Delta u_v(x) = 0.926$  and  $\int_0^1 dx \Delta d_v(x) = -0.341$  [4]. In order to discuss constraints from the RHIC- $\pi^0$  and JLab-E07-011 data on the gluon distribution at relatively large  $x$ , we also show the “first moment” calculated by the integral  $\Delta G(x > 0.1) = \int_{0.1}^1 dx g(x)$  in Table V.

#### A. Impact of RHIC $\pi^0$ data

First, effects of the RHIC  $\pi^0$  data [11] are shown in comparison with the polarized PDFs obtained only by

the DIS data. Using the preliminary PHENIX  $\pi^0$  data of the RHIC RUN-5, we have already shown their impact on the gluon distribution in Ref. [5]. The current analysis uses the published RUN-5 data. Analysis-B results are compared with analysis-A ones in Fig. 2, where the polarized PDFs  $x\Delta u_v$ ,  $x\Delta d_v$ ,  $x\Delta\bar{q}$ , and  $x\Delta g$  and their uncertainties are shown at  $Q^2=1$  GeV<sup>2</sup>. The set A uses only the DIS data and the set B also includes the  $\pi^0$  data as listed in Table II.

The polarized valence-quark distributions  $\Delta u_v(x)$  and  $\Delta d_v(x)$  are not changed even if the RHIC  $\pi^0$  data are included in the analysis. However, there are significant effects on the other distributions, especially on the polarized gluon distribution. The gluon distribution has a huge uncertainty if it is determined only by the DIS data (analysis A); however, the uncertainty band becomes significantly small in the analysis B because of the addition of the  $\pi^0$  data. It is known that gluon-gluon interaction subprocesses dominate the  $\pi^0$ -production cross section especially at small  $p_T$ , so that the  $\pi^0$  data are sensitive to the gluon distribution. We notice that the antiquark uncertainty is slightly reduced in the set B and it is caused by the error correlation between the antiquark and gluon distributions as pointed out in Ref. [5].

The double spin asymmetry for the  $\pi^0$  production indicates a negative value at  $p_T = 2.38$  GeV. It suggests a node type distribution which vanishes at  $x \sim 0.1$  as investigated in Refs. [5, 6, 26]. We also made a global analysis by assigning an initial distribution to a node-type one for  $\Delta g(x)$ . Minimum  $\chi^2$  values per degrees are slightly smaller in the node-type results than the values in the positive ones. In the node-type results of the analysis A, the gluon distribution is positive at  $x > 0.2$  and is slightly negative at small  $x$ . The negative gluon distribution at  $x < 0.1$  becomes smaller in the node-type of the analysis B.

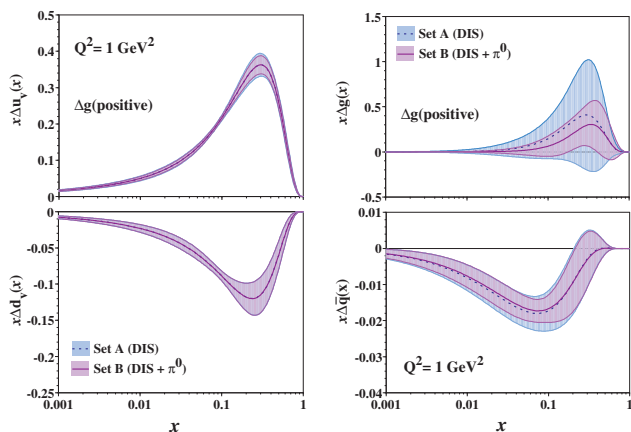


FIG. 2: Comparison of the polarized PDFs between the analyses A and B. They are shown by the dashed and solid curves for the analyses A and B, respectively, at  $Q^2=1$  GeV<sup>2</sup>. Their uncertainties are shown by the shaded bands.

As noticed in Ref. [5], the differences between HERMES ( $Q^2 \simeq 1$  GeV<sup>2</sup>) and COMPASS ( $Q^2 \simeq 6$  GeV<sup>2</sup>) data of  $g_1^d$  at  $x \sim 0.05$  could suggest a positive  $\Delta g(x)$  at large  $x$  ( $> 0.2$ ) although it may be explained by a higher-twist effect [3]. The gluon distribution contributes to  $g_1(x)$  as a NLO effect and the differences could be explained by this NLO effect with  $\Delta g(x) > 0$  at  $x > 0.2$ . In fact, all our global analyses indicate positive distributions at large  $x$ .

The node-type distributions are compared with the positive ones at  $Q^2 = 1$  GeV<sup>2</sup> in Fig. 3. Both distributions are determined by the set-B analysis. It is clear from this figure that the gluon distribution at  $x < 0.1$  cannot be determined by the current data including the RHIC  $\pi^0$  data. In fact, the uncertainty of  $\Delta G$  is large in the node-type distribution and it is obvious that a large contribution comes from the small  $x$  region. Because there is no constraint at small  $x$ , uncertainty reduction of  $\Delta G$  is not very obvious due to the  $\pi^0$  data from the set A to set B as shown in Table IV.

In order to investigate a possible improvement on  $\Delta G$ , we discuss a contribution to the first moment from the region of  $x > 0.1$  in Table V. The relative uncertainties become smaller in the set B from the set A:  $\delta\Delta G(x > 0.1)/\Delta G(x > 0.1) = 1.36 \rightarrow 0.71$  in the positive distribution and  $1.02 \rightarrow 0.77$  in the node one. There are significant reductions in the uncertainties (24%~47%), which suggests that the  $\pi^0$  data impose a significant constraint in the gluon distribution at  $x > 0.1$  in addition to the aforementioned DIS constraint from the scaling violation.

We discuss a comparison with our previous work of

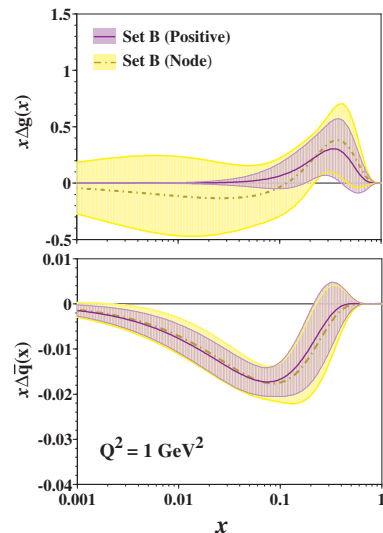


FIG. 3: Polarized antiquark and gluon distributions by the analysis B which includes the RHIC  $\pi^0$ -production data. The distributions and their uncertainties are calculated at  $Q^2 = 1$  GeV<sup>2</sup>. Positive and node-type solutions are shown by the solid and dashed-dot curves, respectively.

AAC06 [5]. The positive distributions of the set B and their uncertainties are compared with the AAC06 results in Fig. 4. There are differences between the used data sets. As explained in Sec. I, additional data, which are not used in the AAC06 analysis, are those of the CLAS [14] and COMPASS [16] collaborations. The PHENIX  $\pi^0$  data [11] were also slightly changed from the preliminary ones at the stage of the AAC06 publication. The used fragmentation functions are also changed from the functions by KKP (Kniehl, Kramer, and Pötter) for the ones by the HKNS07.

As shown in Fig. 4, the distributions and their uncertainties are almost the same. There are slight improvements in the valence-quark and antiquark distributions, which is mainly due to the accurate measurements at medium  $x$  by the CLAS and COMPASS collaborations. The slight reduction in the  $\Delta g(x)$  uncertainty band should come from the error correlation between the quark and gluon distributions. In addition, there are effects due to changes in the  $\pi^0$  data from the preliminary version and in the fragmentation functions. However, these effects are not significant because the distributions themselves are almost the same. We also compared the AAC06 and current distributions for the node type, but they are also almost the same in both distributions and uncertainties.

It should be noted that the description of a  $\pi^0$  production cross section depends much on pion fragmentation functions. Here, the HKNS07 functions [13] are employed in our global analyses for describing the pion cross section. As noted in Ref. [13], there are large uncertainties in the fragmentation functions, especially in the gluon and light-quark functions. Effects of such uncertainties are shown in Fig. 5 together with the RHIC  $\pi^0$ -production data and the asymmetries calculated by using the fragmentation functions of Kretzer and KKP

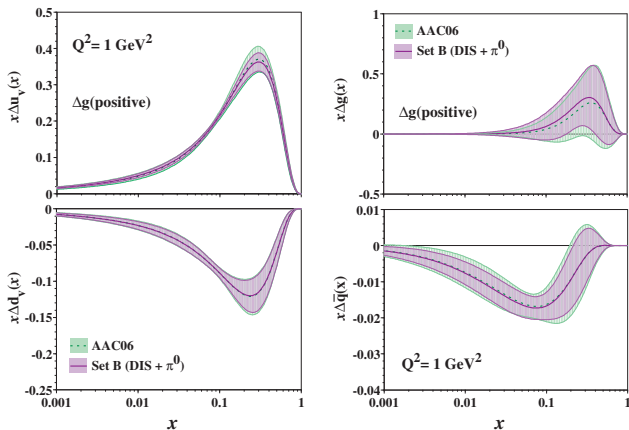


FIG. 4: Comparison of the polarized PDFs between the current analysis B and AAC06 for the positive  $\Delta g(x)$ . They are shown by the dashed and solid curves for the AAC06 and the current analysis (AAC08), respectively, at  $Q^2=1$  GeV $^2$ . Their uncertainties are shown by the shaded bands.

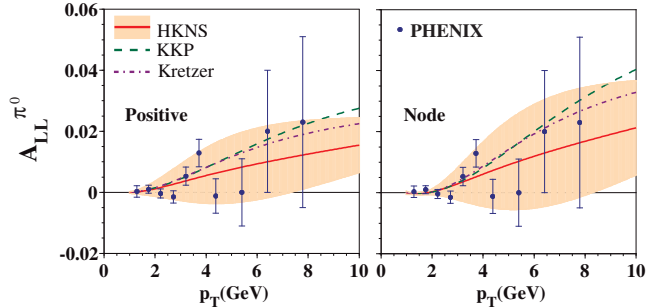


FIG. 5: Set-B results are compared with the PHENIX data in the longitudinal double spin asymmetry of  $\vec{p} + \vec{p} \rightarrow \pi^0 + X$  [11]. The solid curves and the shaded bands indicate theoretical asymmetries and their uncertainties by the HKNS07 fragmentation functions. The results by the KKP and Kretzer fragmentation functions are shown by the dashed and dashed-dot curves, respectively.

as other examples.

The pion production is sensitive to the gluon fragmentation function, which has a large uncertainty because it has been determined mainly by the scaling violation of  $e^+e^- \rightarrow h + X$  data. However, we expect that the situation will improve if the Belle and Babar collaborations provide low-energy  $e^+e^-$  data for clarifying the scaling violation. In our analysis of the pion production, the NLO effects are approximately taken into account as a  $K$ -factor by first calculating the leading-order (LO) cross sections. Therefore, the LO fragmentation functions are used in the analysis, and the asymmetry has the large uncertainty bands as shown in the figure. The gluon fragmentation function is determined more precisely in the NLO [13], so that the uncertainties of  $A_{LL}^{\pi^0}$  are reduced about 1/3. In any case, there are significant effects on the spin asymmetry  $A_{LL}^{\pi^0}$  from the fragmentation functions, which indicates the importance to access the uncertainties from the fragmentation functions in determining the error of  $\Delta g(x)$ .

## B. Impact of JLab-E07-011 data

We discuss the impact of the proposed experiment JLab-E07-011 [17] to measure the structure function  $g_1$  for the deuteron on the determination of the polarized PDFs. The expected E07-011 data [18] in Table II are included in the analysis C. In order to find an improvement to the analysis A with the current DIS data, the polarized PDFs of the analyses C are compared with the analysis-A results in Fig. 6 at  $Q^2=1$  GeV $^2$ . The uncertainties are shown by the shaded bands.

Both distributions are almost the same because the E07-011 data are assumed to be the same asymmetries obtained in the analysis A. The uncertainties are similar in the polarized valence-quark distributions in Fig.

6, whereas the uncertainty of the antiquark distribution becomes smaller in the analysis C than the one of the analysis A. It is also clear that the uncertainty of the gluon distribution is significantly reduced in the analysis C.

There is a possibility that the reduction of the gluon uncertainty due to the E07-011 data could come from the  $Q^2$  dependence in comparison with other data. In order to discuss such a possibility, we show the  $Q^2$  dependence of  $A_1^d$  within the  $x$  range of the E07-011 data in Fig. 7. Two  $x$  ranges are shown. One is at  $0.166 < x < 0.182$  and the other is at  $0.416 < x < 0.50$ . The solid and dashed curves are theoretical set-C results for the positive  $\Delta g(x)$  distribution and an artificial one with  $\Delta g(x) = 0$  at the initial scale  $Q_0^2$ . We notice that differences between these curves are very small in comparison with the experimental errors. The results suggest that the current data should not be accurate enough to probe the polarized gluon distribution from the  $Q^2$  dependence in the  $x$  region,  $0.1 < x < 0.5$ . Therefore, the uncertainty reduction in  $\Delta g$  due to the E07-011 data should come from other sources.

There are two possibilities for the reduction of the gluon uncertainty. First, it could be due to the error correlation between the antiquark and gluon distributions. A more accurate determination of antiquark distributions results in the improvement on the gluon determination through the error correlation between polarized antiquark and gluon distributions.

Second, it could be due to the NLO term with the gluon distribution. In Fig. 8, we show the ratio of the gluon NLO term to  $g_1$ :

$$\frac{1}{g_1(x, Q^2)} \frac{1}{2} \sum_{i=1}^{n_f} e_i^2 \int_x^1 \frac{dz}{z} \Delta C_g(x/z, Q^2) \Delta g(z, Q^2), \quad (5)$$

where  $e_i$  is the quark charge of the flavor  $i$ , and  $\Delta C_g$  is a

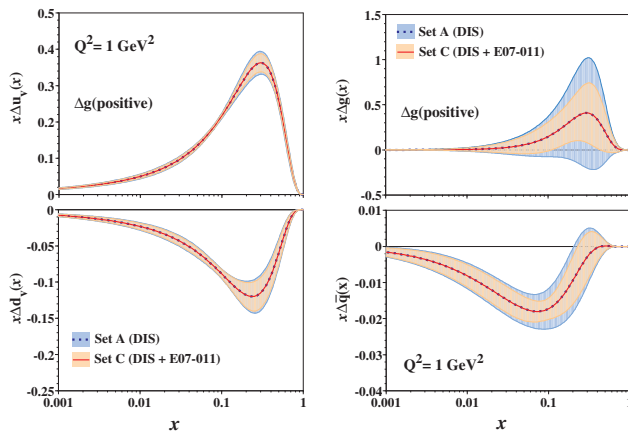


FIG. 6: Comparison of the polarized PDFs between the analyses A and C. They are shown by the dashed and solid curves for the analyses A and C, respectively, at  $Q^2=1$  GeV<sup>2</sup>. Their uncertainties are shown by the shaded bands.

gluonic coefficient function. The ratios are calculated by using the polarized PDFs of the analysis C, and they are shown by solid boxes and triangles. The NLO corrections are calculated at the corresponding experimental  $x$  and  $Q^2$  values. The experimental errors are shown by the ratio

$$\frac{\delta g_1(x, Q^2)}{g_1(x, Q^2)} = \frac{\delta A_1^{exp}(x, Q^2)}{A_1^{exp}(x, Q^2)}, \quad (6)$$

where  $A_1^{exp}(x, Q^2)$  and  $\delta A_1^{exp}(x, Q^2)$  are an experimental spin asymmetry and its error.

It is obvious from Fig. 8 that the gluonic NLO effects are within the experimental errors of the current CLAS data [14] for both proton and deuteron. However, the proposed experiment E07-011 is very accurate, and expected errors are much smaller than the NLO effects shown by the boxes and triangles. It suggests that the E07-011 measurements should be valuable for determining not only the quark and antiquark distributions but also the gluon distribution. However, higher-twist effects become apparent at small  $Q^2$ , so that careful consideration is needed also for them as well as the gluonic NLO contributions if such high-precision data are taken at JLab.

Another global analysis is made by removing only the CLAS data from the data set A, and results indicate that the  $\Delta g(x)$  uncertainty is slightly reduced. From Fig. 8, we find that such a reduction due to the CLAS data is caused mainly by the error correlation between antiquark and gluon distributions because the NLO effects are within the experimental errors. On the other hand, the reduction due to the E07-011 data in Fig. 6 is caused by both the error correlation and the NLO contributions because the NLO effects are much larger than the errors. It is important to find that the E07-011 data are very accurate to probe the higher-order gluonic effects in the

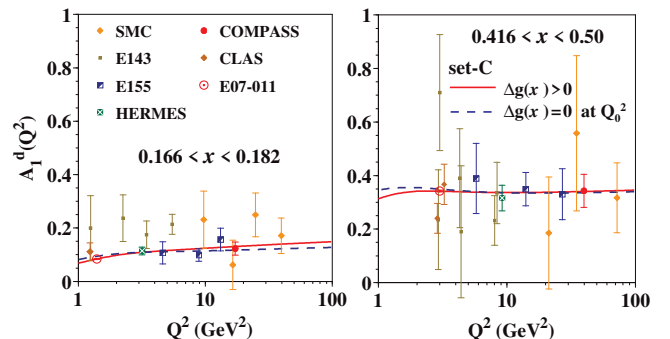


FIG. 7:  $Q^2$  dependence is shown in the spin asymmetry  $A_1$  for the deuteron. The data at  $0.166 < x < 0.182$  and  $0.416 < x < 0.50$  are shown in comparison with the theoretical curves of the analysis C. The solid curves are calculated by the set-C distributions with  $\Delta g(x) > 0$ , and the dashed ones are by the set-C distributions with a different gluon distribution,  $\Delta g(x) = 0$  at  $Q_0^2 = 1$  GeV<sup>2</sup>. The theoretical curves are calculated at  $x = 0.175$  and  $x = 0.45$ .

structure function  $g_1$ .

We comment whether or not such a gluonic NLO term might be effectively absorbed into variations of polarized antiquark distributions because it is generally considered to be difficult to separate both distributions by methods other than the scaling violation. However, it is not the case in our analysis with the E07-011 data. As clearly shown in Fig. 6, the reduction of the gluon uncertainty is much larger than the antiquark one. It cannot be simply explained by the error correlation between the antiquark and gluon distributions. It suggests that the E07-011 data should have a significant impact on the gluon distribution and that the effect should not be absorbed into the antiquark distributions.

Next, we compare the gluon distributions  $\Delta g(x)$  of the analysis C with the analysis-B distributions in Fig. 9. This figure is intended to show the impact of the E07-011 data in comparison with effects of the RHIC  $\pi^0$  data. We found in Fig. 9 that both B and C distributions are similar. However, it should be noted that the positivity condition  $|\Delta g(x)| \leq g(x)$  is not satisfied for the node-type solution in the analyses B and C at large  $x$ . It was difficult to get a converging result within the positivity condition especially for the parameter  $\delta g$ , so that the condition is not imposed in the analysis. We also notice that the relative uncertainties for C are roughly the same with the ones for B. This fact indicates that the effects of the E07-011 data on the determination of  $\Delta g(x)$  are comparable with those of the  $\pi^0$  data.

Mechanisms for the reductions of the gluon uncertainties are completely different in both cases. In the analysis

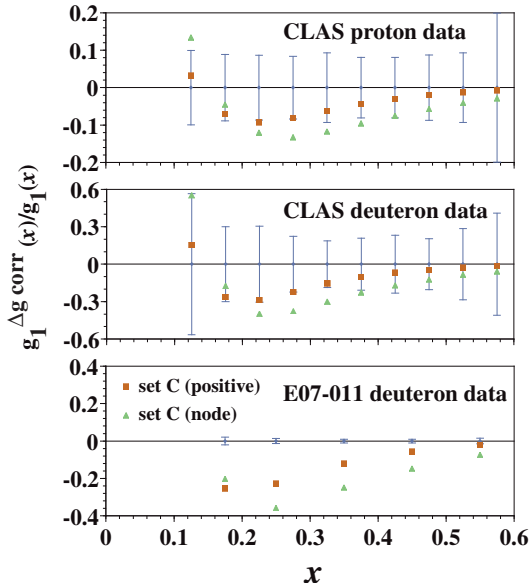


FIG. 8: The ratio of the gluon NLO-correction term to the polarized structure function  $g_1(x, Q^2)$  in Eq. (5). It is compared with experimental errors, which are shown by the ratio  $\delta g_1(x, Q^2)/g_1(x, Q^2)$  in Eq. (6).

B, the reduction is due to the gluon-gluon scattering subprocesses in the  $\pi^0$  production, and it is due to the error correlation and the NLO gluon term of  $g_1$  in the analysis C. Nonetheless, it is noteworthy that high-precision lepton-scattering data can be used for determining the polarized gluon distribution and that the improvement is as good as the current RHIC  $\pi^0$  data.

We comment on possible higher-twist effects. Because the JLab data are taken at relatively small  $Q^2$ , higher-twist corrections may affect the results. Such effects are not included in our leading-twist analysis. There were studies on the higher-twist effects in the structure function  $g_1$  [2, 3]. We also have done a preliminary analysis on such effects; however, they are not precisely determined. Namely, uncertainties of the higher-twist corrections are large, which indicates that they may not be determined by the current experimental data as pointed out in Ref. [2]. If additional parameters are introduced in the higher-twist term, they have very large errors, which makes it difficult to get a reliable polarized PDF set by the current global analysis. We will work on an analysis for obtaining a possible higher-twist correction from the experimental data.

Finally, we discuss the first moment of the polarized gluon distribution,  $\Delta G (= \int_0^1 \Delta g(x) dx)$ . The first moments and their uncertainties are shown in Table IV for all the analyses. We find that the uncertainties become smaller in the set C from the set A:  $\delta \Delta G = 0.81 \rightarrow 0.45$  in the positive distribution and  $1.66 \rightarrow 1.09$  in the node one. In order to investigate a possible constraint on  $\Delta G$  in the large- $x$  region, we also showed the first moment in the kinematical region of  $x > 0.1$  in Table V. The

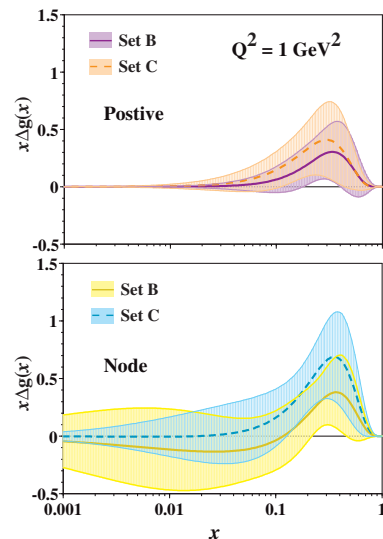


FIG. 9: Polarized gluon distributions and their uncertainties of the analysis C are compared with the ones of the analysis B at  $Q^2=1$  GeV<sup>2</sup>. Both positive and node-type distributions are shown. The set B and C results are shown by the solid and dashed curves.

TABLE VI: The first moment  $\Delta G$  and its uncertainty  $\delta\Delta G$  at  $Q^2 = 1 \text{ GeV}^2$  in the range  $0.1 < x < 1$ . The notations are the same as the ones in Table V.

Function	Set	$\Delta G(x > 0.1)$	$\delta\Delta G(x > 0.1)$	$\frac{\delta\Delta G(x > 0.1)}{\Delta G(x > 0.1)}$
Positive	$C'$	0.49	0.47	0.96
Node	$C''$	0.74	0.52	0.70

relative uncertainties become smaller in the set C from the set A:  $\delta\Delta G(x > 0.1)/\Delta G(x > 0.1) = 1.36 \rightarrow 0.73$  (0.71 in set B) in the positive distribution and  $1.02 \rightarrow 0.54$  (0.77 in set B) in the node one.

The analysis C has been made with the projected E07-011 data which are created so as to agree with the set-A spin asymmetries. In actual experimental measurements, statistical fluctuations exist. Therefore, the reduction of the gluon uncertainty could be overestimated. In order to investigate such a possibility, we tried the following analyses by generating the E07-011 data with two different assumptions:

- Analysis  $C'$ : Projected E07-011 data are obtained by using the node-type distributions in the set A, and then a global analysis is made with positive-type initial distributions.
- Analysis  $C''$ : Projected E07-011 data are obtained by using the positive-type distributions in the set A, and then a global analysis is made with node-type initial distributions.

Analysis results of  $C'$  indicate that the polarized PDFs and their uncertainties are almost the same as the positive-type distributions of the analysis C in the valence-quark and antiquark parts. Determined PDFs of  $C''$  are also almost the same as the node-type ones of the set C. However, the gluon distributions and their uncertainties are slightly modified although  $x$ -dependent functional forms are not changed. The gluon first moments and their uncertainties are shown in Table VI. As expected, the uncertainties become larger than the ones for the analysis C in Table V:  $\delta\Delta G(x > 0.1)/\Delta G(x > 0.1) = 0.96$  [0.73 in set C; 0.71 (B); 1.36 (A)] for the positive type; 0.70 [0.54 in set C; 0.77 (B); 1.02 (A)] for the node type. According to the  $C'$  and  $C''$  results, the improvement from the set A is not as large as the one in the set C. However, it is still comparable with the RHIC improvement in B.

It is important to find that the large uncertainty of  $\Delta G$  is significantly reduced by the proposed E07-011 experiment according to the analysis C (and  $C'$ ,  $C''$ ). The improvement of  $\Delta G$  is especially clear in the integral over the region  $x > 0.1$ . Therefore, the proposed JLab experiment is valuable for the determination of  $\Delta G$  in addition to the quark and antiquark moments. If the polarized lepton scattering data are accurate enough, they can contribute to a better determination of the gluon spin

content. It is interesting to find that the analysis-C uncertainties are almost the same as the ones in the analysis B. However, it should be noted that the uncertainties of the pion fragmentation functions and scale uncertainties are not taken into account in the error estimate of the analysis B.

From these comparisons, we found that the JLab measurements of the the proposed E07-011 can contribute to reducing the uncertainty of the gluon spin content by about 47% in the analysis C (30% in  $C'$  and  $C''$ ). The RHIC  $\pi^0$  measurements also reduce the uncertainty, but the inclusive lepton scattering data are valuable in the sense that they are free from the ambiguities of the fragmentation functions [13].

We should, however, mention that future RHIC experiments will also improve the determination of  $\Delta g(x)$  by measurements of pion, jet, and direct-photon production processes. To be fair with the RHIC-Spin and other high-energy spin projects, it is desirable that a global analysis should be made together with other expected data by the time of the future JLab-E07-011 data. Furthermore, the current estimation would indicate a slightly better determination of  $\Delta g(x)$  from the JLab data because some fluctuations are expected in actual measurements from the central spin asymmetries. However, we believe that our analyses with the expected errors are good enough in comparing the obtained relative errors for the gluon spin content from the DIS and collider data. In this article, we simply showed the role of accurate DIS data, by taking the JLab-E07-011 data as an example, in comparison with the current status because all the expected data are not available for our analysis and also it is not easy to judge which data will be taken before the JLab-E07-011 data.

Because it is one of our purposes to provide a polarized PDF library, which has not been provided since 2003, we did not include preliminary data such as the RHIC run-6 data in our global analyses. In addition, semi-inclusive data are also not included because we focused our analysis on the determination of  $\Delta g(x)$  and the results depend much on used fragmentation functions. In future, we expect to make a more complete analysis including the RHIC run-6 and semi-inclusive data.

#### IV. SUMMARY

We have investigated the impacts of  $\pi^0$ -production data in polarized  $pp$  collisions at RHIC and measurements of  $g_1^d$  in the future JLab experiment E07-011 on the determination of the polarized PDFs, especially the polarized gluon distribution. Global analyses of the polarized DIS were done for determining the polarized PDFs and their uncertainties by using the DIS data on  $g_1$ , the  $\pi^0$  data of the RHIC RUN-5, and the expected JLab-E07-011 data on  $g_1^d$ .

The RHIC  $\pi^0$  data indicated a possibility of a node-type distribution for  $\Delta g(x)$  which changes sign at  $x \sim$

0.1. Accordingly, we made two types of analyses with positive and node-type distributions for  $\Delta g(x)$ . Similar  $\chi_{min}^2$  values were obtained by both analyses although the node-type distributions have slightly smaller  $\chi_{min}^2$ . It suggests that it is difficult to determine a precise gluon distribution from the current data. However, it is interesting to find in our analyses that the distribution  $\Delta g(x)$  is positive at  $x > 0.2$  because of scaling violation in  $g_1$  and  $\pi^0$ -production data. We found a large uncertainty for  $\Delta g(x)$  at small  $x$  ( $< 0.1$ ). The uncertainty of the polarized gluon polarization is significantly reduced by the RHIC  $\pi^0$  data. In particular, the  $\pi^0$  data constrain the gluon moment calculated in the large- $x$  region ( $x > 0.1$ ), and the reduction of the gluon uncertainty is 24%~47% according to our analysis.

There is a clear improvement in the determination of  $\Delta g(x)$  by the future measurements of the E07-011 experiment. It is partially due to the error correlation between the polarized antiquark and gluon distributions. However, the major improvement comes from the fact that the measurements are accurate enough to probe the polarized gluon distribution in the structure function  $g_1$ . Namely, the experimental errors are much smaller than the typical gluonic NLO term in  $g_1$ . The E07-011 data can reduce the uncertainty of the first moment  $\Delta G$  by about 30–47% if only the inclusive DIS data are used in the analysis. This reduction is comparable to the effect of the RHIC RUN-5  $\pi^0$  data. However, the JLab

E07-011 data could have an advantage over the hadron-production data because there is no uncertainty coming from the fragmentation functions and the choice of the hard scale. A better determination of  $\Delta g(x)$  should be also made by future measurements of pion, jet, and direct-photon production processes at RHIC.

Precise DIS and collider measurements are important for determining the polarized PDFs, especially in the polarized gluon distribution. From the analyses B, we provide a code for calculating two sets of optimum polarized PDFs. The set-1 is for the positive-type PDFs in the analysis B, and the set-2 is for the node-type ones also in the analysis B. The code is provided at our web home page [19].

### Acknowledgments

The authors thank N. Saito for useful discussions and comments. They also thank P. Bosted, X. Jiang, and S. Kuhn for communications on JLab experiments and S. Albino, J. Blümlein, H. Böttcher, A. Miller, and Y. Miyachi for communications on the error analysis. They were partially supported by the Grant-in-Aid for Scientific Research from the Japanese Ministry of Education, Culture, Sports, Science, and Technology.

- 
- [1] T. Gehrmann and W. J. Stirling, Phys. Rev. D 53 (1996) 6100; G. Altarelli, R. D. Ball, S. Forte, and G. Ridolfi, Nucl. Phys. B496 (1997) 337; L. E. Gordon, M. Goshatpour, and G. P. Ramsey, Phys. Rev. D 58 (1998) 094017; B. Adeva *et al.* (Spin Muon Collaboration (SMC)), Phys. Rev. D 58 (1998) 112002; M. Glück, E. Reya, M. Stratmann, and W. Vogelsang, Phys. Rev. D 63 (2001) 094005; D. de Florian, G. A. Navarro, and R. Sassot, Phys. Rev. D 71 (2005) 094018; C. Bourrely, J. Soffer, and F. Buccella, Eur. Phys. J. C 41 (2005) 327.
- [2] J. Blümlein and H. Böttcher, Nucl. Phys. B 636 (2002) 225.
- [3] E. Leader, A. V. Sidorov, and D. B. Stamenov, Phys. Rev. D 73 (2006) 034023; 75 (2007) 074027.
- [4] Y. Goto *et al.* (Asymmetry Analysis Collaboration (AAC)), Phys. Rev. D 62 (2000) 034017; M. Hirai, S. Kumano, and N. Saito (AAC), Phys. Rev. D 69 (2004) 054021.
- [5] M. Hirai, S. Kumano, and N. Saito (AAC), Phys. Rev. D 74 (2006) 014015.
- [6] D. de Florian, R. Sassot, M. Stratmann, and W. Vogelsang, arXiv:0804.0422 [hep-ph].
- [7] A. Airapetian *et al.* (HERMES Collaboration), Phys. Rev. Lett. 84 (2000) 2584; P. Liebing, AIP Conf. Proc. 915 (2007) 331.
- [8] B. Adeva *et al.* (SMC), Phys. Rev. D 70 (2004) 012002.
- [9] E. S. Aggev *et al.* (COMPASS Collaboration), Phys. Lett. B 633 (2006) 25.
- [10] M. Alekseev *et al.* (COMPASS), arXiv:0802.3023 [hep-ex].
- [11] A. Adare *et al.* (PHENIX Collaboration), Phys. Rev. D 76 (2007) 051106.
- [12] B. I. Abelev *et al.* (STAR Collaboration), Phys. Rev. Lett. 97 (2006) 252001; 100 (2008) 232003.
- [13] M. Hirai, S. Kumano, T.-H. Nagai, and K. Sudoh, Phys. Rev. D 75 (2007) 094009; M. Hirai, S. Kumano, M. Oka, and K. Sudoh, Phys. Rev. D 77 (2008) 017504.
- [14] K. V. Dharmawardane *et al.* (CLAS Collaboration), Phys. Lett. B 641 (2006) 11.
- [15] A. Airapetian *et al.* (HERMES), Phys. Rev. D 75 (2007) 012007.
- [16] V. Y. Alexakhin *et al.* (COMPASS), Phys. Lett. B 647 (2007) 8.
- [17] E. Brash *et al.*, JLab experiment E07-011, [http://www.jlab.org/exp\\_prog/proposals/07/PR-07-011.pdf](http://www.jlab.org/exp_prog/proposals/07/PR-07-011.pdf).
- [18] Xiaodong Jiang, personal communications.
- [19] AAC home page: <http://spin.riken.bnl.gov/aac/>.
- [20] K. Boyle, Workshop on Gluon Polarization in the Nucleon, Urbana, Illinois, USA, June 16-17, 2008.
- [21] M. Glück, E. Reya, and A. Vogt, Eur. Phys. J. C 5 (1998) 461.
- [22] S. Kumano, Phys. Rept. 303 (1998) 183; G. T. Garvey and J.-C. Peng, Prog. Part. Nucl. Phys. 47 (2001) 203.
- [23] M. Hirai, S. Kumano, and M. Miyama, Comput. Phys. Commun. 108 (1998) 38; 111 (1998) 150; M. Miyama and S. Kumano, Comput. Phys. Commun. 94 (1996) 185.
- [24] For example, see <http://wwwasdoc.web.cern.ch/wwwasdoc/minuit/node33.html>, <http://ccwww.kek.jp/pdg/2007/>

reviews/statrpp.pdf.

- [25] J. Pumplin *et al.*, JHEP, 0207 (2002) 012; A. D. Martin *et al.*, Eur. Phys. J. C 28 (2003) 455.
- [26] B. Jäger, M. Stratmann, S. Kretzer, and W. Vogelsang,

Phys. Rev. Lett. 92 (2004) 121803; M. Hirai and K. Sudoh, Phys. Rev. D 71 (2005) 014022.